DYRK1A regulates B cell acute lymphoblastic leukemia through phosphorylation of FOXO1 and STAT3

Rahul S Bhansali, Malini Rammohan, Paul Lee, Anouchka Laurent, Qiang Wen, Praveen Suraneni, Bon Ham Yip, Yi-Chien Tsai, Silvia Jenni, Beat Bornhauser, Aurélie Siret, Corinne Fruit, Alexandra Pacheco-Benichou, Ethan Harris, Thierry Besson, Benjamin J Thompson, Young Ah Goo, Nobuko Hijiya, Maria Vilenchik, Shai Izraeli, Jean-Pierre Bourquin, Sebastien Malinge, and John D Crispino*

Corresponding Author:
John D Crispino
St. Jude Children's Research Hospital
262 Danny Thomas Place, MS341
Memphis, TN 38105
Phone: 901-595-7511
Email: j-crispino@northwestern.edu; john.crispino@stjude.org

Supplementary Methods

Cancer Cell Line Encyclopedia (CCLE) Gene Expression Analysis. CCLE (Broad Institute, Cambridge, MA)(21) was searched for "DYRK1A," "FOXO1," and "STAT3." Data from "mRNA Expression (RNAseq)" and "Copy Number" datasets were extracted and analyzed for differential gene expression.

St. Jude GenomePaint Query. The Pan-ALL dataset in St. Jude GenomePaint(21) was queried for *DYRK1A*, *FOXO1*, and *STAT3.* Kaplan-Meier curves were plotted by stratification into quartiles based on gene expression.

Colony replating assays. For colony replating assays, bone marrow was harvested from C57BL/6 mice 4-6 weeks of age. B cell precursors were isolated by collecting the B220-positive and lineage-negative fraction using the mouse hematopoietic progenitor (Stem) Cell Enrichment Set (BD) with biotin anti-mouse lineage panel consisting of TER-119, CD11b, Ly-6G/Ly-6C (Gr-1), and CD3e biotin-conjugated monoclonal antibodies. 200e3 cells transduced with MIGR1-*Dyrk1a* or MIGR1 were plated into M3630 medium and were incubated at 37°C. At 1 week timepoints, colonies were counted, harvested, and replated in equal quantities to assess for clonality.

Complete blood counts. Blood (100µL) was collected from the tail vein in EDTA-coated tubes and analyzed by a Hemavet 850 complete blood counter.

Cell culture. B-ALL cell lines (MHH-CALL-4, MHH-CALL-2, MUTZ-5, 697, Nalm-6, REH, RCH-ACV) were purchased from Deutsche Sammlung von Mikroorganismen und Zellkulturen (DSMZ), confirmed to be free of mycoplasma contamination by PCR, and authenticated by a human 9-marker STR profile test (IDEXX BioResearch). Cells were cultured in RPMI supplemented with 10% FBS (697, Nalm-6, RCH-ACV) or 20% FBS (MHH-CALL-4, MHH-CALL-2, MUTZ-5, REH), 2mM L-glutamine, and penicillin/streptomycin (GIBCO). Human Ph-like ALL samples were obtained from the PROPEL repository (St. Jude Children's Hospital). Briefly, 1e6 cells were transplanted into NSG mice. After 1 month of expansion, leukemic cells were harvested from bone marrow using human CD19 and human CD45 selection EasySep kits (Stem Cell Technologies) and then cultured ex vivo. For pre-B cell cultures, bone marrow cells were collected from C57BL/6 mice. Lineage-negative cells were negatively selected from suspension of bone marrow using the EasySep kit (Stem Cell Technologies) and grown in the presence of OP9 mouse stromal cells (ATCC) in cytokine-supplemented (10ng/μL mSCF, 5ng/μL hFlt3, and 1ng/μL mIL7 [PeproTech]) OP9 co-culture media (Alpha-MEM supplemented with 10% FBS [HyClone], 2mM L-glutamine, 1x Primocin [Invivogen], and Gentamicin [GIBCO]). Cells were passaged every 4 days, and confirmation of pre-B cell immunophenotype was performed by flow cytometric identification of the IgM^-, $B220^+$, $CD43^{low/-}$ population. OP9 cells were cultured alone in Alpha-MEM supplemented with 20% FBS (HyClone), 2mM L-glutamine, 1x Primocin (Invivogen), Gentamicin (GIBCO).

For drug treatment experiments, pre-B cells were harvested and passed through a 40μM filter to remove OP9 stromal cells and equilibrated to cytokine-supplemented (10ng/μL mSCF, 5ng/μL hFlt3, and 5ng/μL mIL7 [PeproTech]) pre-B cell media (DMEM supplemented with 10% FBS

[Hyclone], 2mM L-glutamine, 10mM Hepes, 1mM sodium pyruvate, 1x Primocin [InvivoGen] and 55μM beta-mercaptoethanol) and passaged every 2 days.

qRT-PCR. Total RNA was isolated from murine leukemic cells, murine pre-B cells, or B-ALL cell lines (Nalm-6 and 697) using RNeasy kits (QIAGEN) and reverse transcribed using SuperScript III First Strand Synthesis Kits (Life Technologies). Real-time PCR was performed using PerfeCTa SYBR Green (Quanta Biosciences) and gene-specific primers. Data were quantified using $2^{-\Delta\Delta Ct}$ method.

Western blotting. Whole cell lysis was performed with TENT buffer (50mM Tris, pH 8.0, 2mM EDTA, 150mM NaCl, 1% Triton X-100) supplemented with 2mM NaF, 2mM $NaVO_3$, 2mM Sodium Pyrophosphate, 2mM beta-glycerophosphate, and 1x cOmplete protease inhibitor cocktail (Roche) or RIPA buffer (ThermoFisher Scientific) supplemented with Halt Protease Inhibitor Cocktail (ThermoFisher Scientific) for 30 minutes on ice. Debris was cleared by centrifugation at 21000g for 10 minutes at 4°C. Low-input Western blots were performed as previously described(83) by sorting 50e3 cells directly into 10% TCA and incubating on ice for 15 minutes. Lysates were clarified by centrifugation and washed twice in -20°C acetone. Pellets were resuspended in 9M Urea, 1% Triton X-100, and 1% DTT. Subcellular fractionation was performed by lysis with Harvest buffer (10mM HEPES, pH 7.9, 50mM NaCl, 0.5M Sucrose, 0.1mM EDTA, and 0.5% Triton X-100) supplemented with 1mM DTT, 2mM NaF, 2mM $NaVO_3$, 2mM Sodium Pyrophosphate, 2mM beta-glycerophosphate, and 1x cOmplete protease inhibitor cocktail (Roche) for 10 minutes on ice. Nuclei were pelleted at 720g for 10 minutes and supernatant (cytoplasmic fraction) was cleared by centrifugation. Nuclear/chromatin-bound

pellet was washed in Buffer A (10mM HEPES, pH 7.9, 10mM KCl, 0.1mM EGTA, and 0.1mM EDTA) supplemented with 1mM DTT, 2mM NaF, 2mM $NaVO_3$, 2mM Sodium Pyrophosphate, 2mM beta-glycerophosphate, and 1x cOmplete protease inhibitor cocktail (Roche). Pellet was then lysed in Buffer C (10mM HEPES, pH 7.9, 500nM NaCl, 0.1mM EGTA, 0.1mM EDTA, 0.1% NP-40, and 250U/mL Benzonase) supplemented with 1mM DTT, 2mM NaF, 2mM $NaVO_3$, 2mM Sodium Pyrophosphate, 2mM beta-glycerophosphate, and 1x cOmplete protease inhibitor cocktail (Roche) by vortexing for 15 minutes at 4°C. Lysates were cleared by centrifugation and supernatant (nuclear/chromatin-bound fraction) was kept for use. Lysates were denatured in LDS sample loading buffer (Life Technologies) at 95°C for 5 minutes and electrophoresed on 4-15% Mini-Protean TGX gels (BioRad). Proteins were transferred to PVDF membranes (EMD Millipore) and probed with primary antibodies against DYRK1A, Cyclin D3, phospho-Cyclin D3 T283, FOXO1, phospho-FOXO1 S329, TBP, phospho-STAT3 S727, phospho-STAT3 Y705, STAT3 and HSC70. Actin was detected using HRP-conjugated primary antibody. All Western blots were detected with HRP-conjugated secondary antibodies and visualized with ECL substrate (GE Healthcare) or SuperSignal West Substrate (ThermoFisher Scientific) using HyBlot CL radiography film (Denville), with the exception of panels 4B, 4C, 7B, and 7C, which were detected with IRDye secondary antibodies (LI-COR) and visualized with Odyssey CLx Imaging System (LI-COR). Antibodies are described in detail in Supplementary Table S9. Densitometry values were calculated using ImageJ software.

Retroviral production and transduction. Platinum-E or Platinum-A cells (Cell Biolabs) were grown to 70-80% confluence in antibiotic-free medium in 10-cm dishes for mouse or human cell experiments, respectively. They were transfected with 10μg of retroviral plasmid (MIGR1,

MIGR1-*Dyrk1a*^{WT}, MIGR1-*Dyrk1a*^{K188R}, MIGR1-*BCR-ABL* [p190], MIGR1-*Cre*, MSCV-puro, MSCV-puro-*STAT3*^{WT}, MSCV-puro-*STAT3*^{S727A}, MSCV-puro-*STAT3*^{S727D}, MSCV-puro-*STAT3*^{S727E}) using Xtreme Gene 9 (Roche). Fresh medium was replaced after 12 hours, and viral supernatant was collected at 24 and 48 hours after transfection and 0.45μM filtered to remove cell debris. Virus was concentrated by adding 320μg/mL polybrene and centrifugation at 10000g for 10 minutes at 4°C. Cells were transduced by adding concentrated virus resuspended in complete culture medium and 25mM Hepes and centrifugation at 2500rpm for 90 minutes at 32°C. Cells were then incubated for an addition 4-8 hours at 37°C before replacing medium.

Lentiviral production and transduction for shRNA mediated knockdown. 293T cells (ATCC) were grown to 70-80% confluence in antibiotic-free medium in 10-cm dishes. Cells were then transfected in 1:9:9 ratio with packaging plasmids (pMD2.G, psPAX2) and pTRIPZ inducible shRNAs made available by Dharmacon (scrambled, DYRK1A_1 [V3THS_376671] or DYRK1A_2 [V3THS_376672]) using Xtreme Gene 9 (Roche). Fresh medium was replaced after 12 hours, and viral supernatant was collected at 24 and 48 hours after transfection and 0.45μM filtered to remove cell debris. Viral particles were concentrated by ultracentrifugation at 100,000g for 1 hour and 30 minutes at 4°C. Hematopoietic cells were transduced by adding concentrated virus resuspended in complete culture medium with 25mM Hepes and 10μg polybrene and centrifugation at 2500rpm for 90 minutes at 32°C twice, with an hour of incubation at 37°C between the spins. shRNA expression was induced through addition of 0.5μg/μl doxycycline for 3 days, after which cells were harvested for analysis.

CRISPR/Cas9 targeting of *DYRK1A*. To achieve gene knockout, 2e6 MUTZ-5 cells were mixed with 450pmol of *DYRK1A*-specific sgRNAs (predesigned Gene Knockout Kit v2, Synthego) and 50pmol of Cas9 2NLS Nuclease (Synthego). Same number of cells were also mixed with 450pmol of non-targeting sgRNA (Synthego) and 50pmol of Cas9 2NLS Nuclease to serve as a control. The cells were then resuspended in 100ul of T Buffer (ThermoFisher Scientific) for electroporation in the Neon Transfection System (ThermoFisher Scientific). Cells were loaded in 100ul tips and electroporated according to the manufacturer's instructions using the setting of 1350 volts, 30ms width, and 1 pulse. Following electroporation, cells were recovered in RPMI (ThermoFisher Scientific) containing 20% FBS (ThermoFisher Scientific) for 24 hours before undergoing another round of electroporation to increase the knockout efficiency. Cells were then harvested for Western blotting 24 hours later.

In vitro kinase assay. Nonradioactive kinase assays were performed as previously described(16, 84). 293T cells were transfected with 1098 pcDNA GFP FKHR WT or S329A and lysed 2 days later for immunoprecipitation with GFP-Trap®-MA beads (ChromoTek). Bead-bound FOXO1 was washed extensively and then added to kinase reactions containing recombinant GST-hDYRK1A (ThermoFisher Scientific), ATP-gamma-S (Abcam), and kinase assay buffer (40mM Tris, pH 7.5, 10mM $MgCl_2$, and 50mM NaCl). Reactions were mixed in a ThermoMixer (Eppendorf) at 30°C for 45 minutes. 2.5mM P-nitrobenzyl mesylate (PNBM; Abcam) was added to alkylate thiophosphates. Western blot was then performed on reactions and probed with anti-thiophosphate ester antibody.

Mitochondrial Fractionation. 20e6 cells were harvested for mitochondria isolation using Mitochondria Isolation Kit for Mammalian Cells (8984, ThermoFisher Scientific). Isolated mitochondria were directly lysed in SDS-PAGE buffer for western blot and subsequent analysis was performed as described above.

Fluorescence microscopy. The plasmid 1098 pcDNA GFP FKHR was a gift from William Sellers(85) (Addgene plasmid #9022; http://n2t.net/addgene:9022; RRID:Addgene 9022)**.** Site-directed mutagenesis was performed using QuikChange kits (Agilent) and confirmed with DNA sequencing. The plasmids were transiently transfected into primary murine pre-B cells using Cell Line Nucleofector Kit V and Nucleofector 2b Device (Lonza) with program V-001. Transfected cells were cultured for 48 hours and then treated with 2.5μM EHT 1610 or DMSO for 4 hours before fixation and 10μg/mL Hoechst 33342 for 1 hour before fixation. Cells were then attached to the cover slip coated with 25 μg/ml of fibronectin for 1hr at 37°C. Cells were then stained with Hoechst (Sigma-Aldrich) for 1hr, washed with phosphate buffer saline and fixed with 4% paraformaldehyde for 30 minutes. Fluorescent images were obtained using the Nikon A1R+ confocal microscope under a 60× Plan-Apochromat oil immersion lens.

Global phosphoproteomics. Wild-type murine pre-B cells were cultured as described in Methods. Cells were treated for 2 hours with 2μM EHT 1610 or DMSO in the presence of MG-132 (Sigma-Aldrich). Cells were pelleted and washed in PBS. Pellets were then resuspended in Urea lysis buffer (8M Proteomics Grade Urea [Sigma-Aldrich], 20mM Hepes [pH 8.0], 1μM sodium orthovanadate, 2μM sodium pyrophosphate, and 2μM beta-glycerophosphate). Suspensions were then sonicated with a setting of 5 with 15-20 bursts at 2 seconds on/2 seconds

off. The lysate was collected following centrifugation, and 1mg of protein from each sample was used for digestion followed by phosphopeptide enrichment. The samples were reduced with DTT (5mM, 45°C, 30 min) followed by alkylation with 2-chloroacetamide (65mM, room temperature, 30 min). Samples were diluted with 100mM ammonium bicarbonate to reduce the urea concentration to <1.2M. Digestion was initiated with the addition of trypsin (1:50 W:W ratio; Promega) and incubated overnight at 37°C with constant shaking on a Thermomixer. Digestion was stopped by adding TFA (final concentration of 0.1%). Samples were desalted using SepPak C18 cartridges (Waters) following manufacturer's protocol and completely dried using vacufuge (Eppendorf).

Titanium dioxide (TiO_2)-based metal oxide affinity chromatography was used for phosphopeptide enrichment. The Titansphere Phos-TiO kit was purchased from GL Sciences Inc., and phosphopeptide enrichment was performed according to the manufacturer's protocol with minor modifications. Briefly, a spin tip column packed with 6mg of TiO_2 beads was conditioned with buffer A (0.5% TFA/80% acetonitrile) and equilibrated with buffer B (25% lactic acid/0.5% TFA/60% acetonitrile solution. Tryptic peptides were dissolved in buffer B and loaded onto the column. After several washings with buffers A and B to remove non-phosphorylated peptides, phosphopeptides were eluted serially with 100µl each of 5% ammonium hydroxide and 5% pyrrolidine solutions. Eluents were combined and cleaned up using SepPak C18 cartridge (Waters) and completely dried.

Tandem Mass Tag labeling: The Tandem Mass Tag (TMT) labeling was performed using TMT-6plex isobaric labeling kit (ThermoFisher Scientific). The labeling of the sample was performed according to the manufacturer's protocol. Briefly, dried phosphopeptides were solubilized with 100µl of 0.1M TEAB solution. Samples 1-6 were labeled with TMT channels.

TMT reagents were reconstituted in 41µl of anhydrous acetonitrile and peptides were transferred to the TMT reagent vial and incubated at room temperature for 1 hour. The reaction was quenched by adding 8µl of 5% hydroxylamine and incubating it for further 15 minutes. The samples were then combined and dried. Prior to MS analysis, two-dimensional separation of the samples was performed. For the 1st dimension, an offline fractionation using high pH reverse phase fractionation kit into 8 fractions was performed following the manufacturer's protocol (Pierce, Cat #84868). Fractions were dried and reconstituted in 10µl of loading buffer (0.1% formic acid and 2% acetonitrile). Liquid Chromatography-mass spectrometry analysis (LC-Multinotch MS3): Orbitrap Fusion (ThermoFisher Scientific) and RSLC Ultimate 3000 nano-UPLC (Dionex) were used to acquire the data. 2µl of each fraction was resolved in the 2nd dimension on a nano-capillary reverse phase column (Acclaim PepMap C18, 2 micron, 75µm i.d. x 25 cm, ThermoFisher Scientific) using a 0.1% formic/acetonitrile gradient at 300nl/minute (2-22% acetonitrile in 50 minutes;22-32% acetonitrile in 25 minutes; 10 minutes wash at 90% followed by 25 minutes re-equilibration) and directly sprayed on to Orbitrap Fusion using EasySpray source (ThermoFisher Scientific). Mass spectrometer was set to collect one MS1 scan (Orbitrap; 120K resolution; AGC target $2x10^5$; max IT 100 ms) followed by data-dependent, "Top Speed" (3 seconds) MS2 scans (High-energy C-trap dissociation; 60K resolution; NCD 35; AGC $5x10^4$; max IT 250 ms).

Proteome Discoverer (v1.4 ThermoFisher Scientific) was used for data analysis. MS2 spectra were searched against mouse protein database (release 2014-01; 51629 sequences including Common Contaminant list) using the following search parameters: MS1 and MS2 tolerance were set to 10 ppm and 0.1 Da, respectively; carbamidomethylation of cysteines (57.02146 Da) and TMT labeling of lysine and N-termini of peptides (229.16293 Da) were

considered static modifications; oxidation of methionine (15.9949 Da), deamidation of asparagine and glutamine (0.98401 Da) and phosphorylation on serine, threonine and tyrosine were considered variable. Identified proteins and peptides were filtered to retain only those that passed ≤1% FDR threshold. PhosphoRS and Reporter ion quantifier modules of Proteome Discoverer were used to determine the phosphosite localization probabilities and extract reporter ion-based quantitation, respectively.

Kinase assay-linked phosphoproteomics. Kinase assay procedure was modified from the kinase assay-linked phosphoproteomics method(86, 87) with changes described below. Murine pre-B cells pellets were collected and resuspended in a lysis buffer containing 8M proteomics grade Urea (Sigma-Aldrich), 50mM Tris-HCl, 75mM NaCl, and 25U/mL Benzonase (EMD Millipore). Suspensions were sonicated with a setting of 5 for 15-20 bursts at 2 seconds on/2 seconds off. Protein concentration in the supernatants was determined by a 660nm assay (ThermoFisher Scientific).

Four milligrams of total protein per sample were prepared for phosphoproteomics analysis. Lysates were treated with 1mM 5'-(4-fluorosulfonylbenzoyl)adenosine (FSBA) (1 hour, 30C) to inhibit endogenous kinase activity. Excess FSBA was washed out using 3 kDa Amicon filters (EMD Millipore). Samples were then incubated at 50°C with 5mM DTT for 30 minutes, cooled to room temperature, and alkylated with 15mM iodoacetamide for 60 minutes in the dark. First digestion was performed with rLys-C (1:200 w:w, Promega) overnight at 37°C in order to maintain the DYRK1A phosphorylation motif with contains arginine. 0.5% TFA was added to halt the reaction and debris was cleared. Samples were desalted using SepPak C18 cartridges (Waters) with two elution steps using 0.1% TFA in 50% Acetonitrile and 0.1% TFA in

80% Acetonitrile. Eluents were completely dried with SpeedVac centrifugation. Peptides were incubated with Lambda phosphatase (NEB) for 2 hours at 5U/µg. Phosphatase was deactivated by heating for 1 hour at 65°C in the presence of 10mM sodium orthovanadate, 50mM sodium fluoride, 2mM beta-glycerophosphate, and 2mM sodium pyrophosphate. Kinase assay was then performed by adding 1x Kinase buffer (40mM Tris-HCl, 10mM $MgCl_2$, 50mM NaCl), 250µM ATP, 1µg recombinant NFATc1 (Sigma-Aldrich), and ≤1% protein weight recombinant DYRK1A (ThermoFisher Scientific) and incubated for 2.5 hours at 30°C. The reaction was quenched by adding EDTA to 20mM. A second digestion was performed with addition of acetonitrile to 10% followed by sequencing-grade trypsin (1:50 w:w, Promega), and the reaction was incubated overnight at 37°C. Complete digestion was confirmed by running aliquot on a Western blot and Imperial staining (ThermoFisher Scientific). Samples were desalted using SepPak C18 cartridges (Waters) with two elution steps using 0.1% TFA in 50% Acetonitrile and 0.1% TFA in 80% Acetonitrile. Eluents were completely dried with SpeedVac centrifugation.

Phosphopeptides were enriched using bulk 5um Titanosphere TiO_2 beads (GL Sciences) following the procedure previously described with minor modifications(88, 89). Desalted peptides from 4 mg of lysate were resuspended in a solution of 65% ACN, 2% TFA, and saturated glutamic acid. Each sample was mixed with 3mg of TiO_2 beads and shaken for 20 minutes at room temperature. Beads with bound phosphopeptides were washed by shaking twice in 65% ACN, 0.5% TFA for 10 minutes, then washed twice more in 65% ACN, 0.1% TFA for another 10 minutes. Phosphopeptides were eluted by shaking 20 minutes in 300 mM NH_4OH/50% ACN, then twice with 500 mM NH_4OH/60% ACN. The eluates from these three steps were combined and acidified with formic acid (FA).

High pH reverse-phase (HpRP) chromatography in a solid-phase extraction format was used to fractionate the phosphopeptides as previously described(88, 90). All solvents used for HpRP fractionation contained aqueous 10mM NH_4HCO_3 at pH 10, with acetonitrile added as indicated. Peptides were pH-adjusted by adding 100 mM NH_4HCO_3 to a final pH of 10, then loaded onto hydrophilic-lipophilic balanced (HLB) reversed-phase Sep-Pak cartridges (Waters). Cartridges were rinsed with 1% ACN /99% 10 mM ABC prior to eluting peptides with 5%, 10%, 15%, 20%, 25%, 30%, 35%, and 80% ACN. The eight fractions were concatenated to four fractions per sample. The 5% ACN fraction was mixed with the 25% ACN fraction, 10% ACN with 30% ACN, 15% ACN with 35% ACN, and 20% ACN with 80% ACN. After acidification with FA and vacuum drying to remove ACN, all fractions were desalted by C18 spin column (ThermoFisher Scientific) prior to LC-MS/MS analysis.

Desalted phosphopeptide-enriched fractions were resuspended in 5% ACN/0.1% FA. Nano LC-MS/MS analyses were performed with a 75 μm x 10.5 cm PicoChip column packed with 3 μm Reprosil C18 beads. A 150 μm x 3 cm trap packed with 3um beads was installed in-line. Solvent A consisted of 0.1% FA in water and solvent B was 0.1% in ACN. Peptides were trapped at 5 μL/minute for 5 min, then separated at a flow rate of 300 nL/minute with a gradient from 5% to 30% B for 100 minutes. After a 4 minute ramp to 60% B, the column was washed at 95% B and re-equilibrated to 5% B with a total analysis time of 120 min.

The LC was coupled by electrospray to Q Exactive™ HF Hybrid Quadrupole-Orbitrap™ Mass Spectrometer (ThermoFisher Scientific) operating in data-dependent MS/MS mode with a top-15 method. Dynamic exclusion was set to 20 s and charge 1+ ions were excluded. MS^1 scans were collected from 300-2000 *m/z* with resolving power equal to 60,000. The MS^1 AGC was set to $3x10^6$. Precursors were isolated with a 2.0 m/z isolation width, and the HCD normalized

collision energy was set to 30%. The MS^2 AGC was set to $1x10^5$ with the resolving power set at 30,000.

LC-MS results were searched in MaxQuant 1.6.0.16 against the SwissProt mouse database (version downloaded 10/2017) and a list of common contaminants. Cysteine carbamidomethylation was a fixed modification, and oxidized methionine was a variable modification. Phosphorylation of S, T, and Y residues were allowed for enriched fractions. Two missed cleavages were allowed, and Trypsin/P was selected as the enzyme. The "first search" precursor mass tolerance was set to 20 ppm, "main search" tolerance was set to 6 ppm, and fragment mass tolerance was set to 50 ppm. A 1% FDR was applied at the peptide and protein level.

Phosphopeptides were quantified in a label-free manner. MaxQuant-derived precursor intensities were converted to log_2-scale fold changes. From these, robust z-scores (x-median fold change/median absolute deviation) were calculated to compare kinase treated cells vs. vehicle treated. Phosphorylation was considered confidently localized to a specific amino acid when scored with 75% probability or better.

Bioinformatic analysis of phosphoproteomic studies. For bioinformatic analysis, peptides with 1.5-fold change in phosphorylation were utilized. Both global and kinase assay-directed phosphoproteomics datasets were entered into String database for KMEANS clustering of interactome and identification of GO biological processes and KEGG pathway annotations.

Supplementary References

82. Fischer U, Forster M, Rinaldi A, Risch T, Sungalee S, Warnatz HJ, et al. Genomics and drug profiling of fatal TCF3-HLF-positive acute lymphoblastic leukemia identifies recurrent mutation patterns and therapeutic options. *Nature genetics.* 2015;47(9):1020-9.

83. Signer RA, Qi L, Zhao Z, Thompson D, Sigova AA, Fan ZP, et al. The rate of protein synthesis in hematopoietic stem cells is limited partly by 4E-BPs. *Genes Dev.* 2016;30(15):1698-703.

84. Allen JJ, Li M, Brinkworth CS, Paulson JL, Wang D, Hubner A, et al. A semisynthetic epitope for kinase substrates. *Nat Methods.* 2007;4(6):511-6.

85. Nakamura N, Ramaswamy S, Vazquez F, Signoretti S, Loda M, and Sellers WR. Forkhead transcription factors are critical effectors of cell death and cell cycle arrest downstream of PTEN. *Mol Cell Biol.* 2000;20(23):8969-82.

86. Xue L, Arrington JV, and Tao WA. Identification of Direct Kinase Substrates via Kinase Assay-Linked Phosphoproteomics. *Methods Mol Biol.* 2016;1355:263-73.

87. Xue L, Wang WH, Iliuk A, Hu L, Galan JA, Yu S, et al. Sensitive kinase assay linked with phosphoproteomics for identifying direct kinase substrates. *Proc Natl Acad Sci U S A.* 2012;109(15):5615-20.

88. Schunter AJ, Yue X, and Hummon AB. Phosphoproteomics of colon cancer metastasis: comparative mass spectrometric analysis of the isogenic primary and metastatic cell lines SW480 and SW620. *Anal Bioanal Chem.* 2017;409(7):1749-63.

89. Yue X, Schunter A, and Hummon AB. Comparing multistep immobilized metal affinity chromatography and multistep TiO2 methods for phosphopeptide enrichment. *Anal Chem.* 2015;87(17):8837-44.

90. Yue XS, and Hummon AB. Combination of multistep IMAC enrichment with high-pH reverse phase separation for in-depth phosphoproteomic profiling. *J Proteome Res.* 2013;12(9):4176-86.

Supplementary Figures and Legends

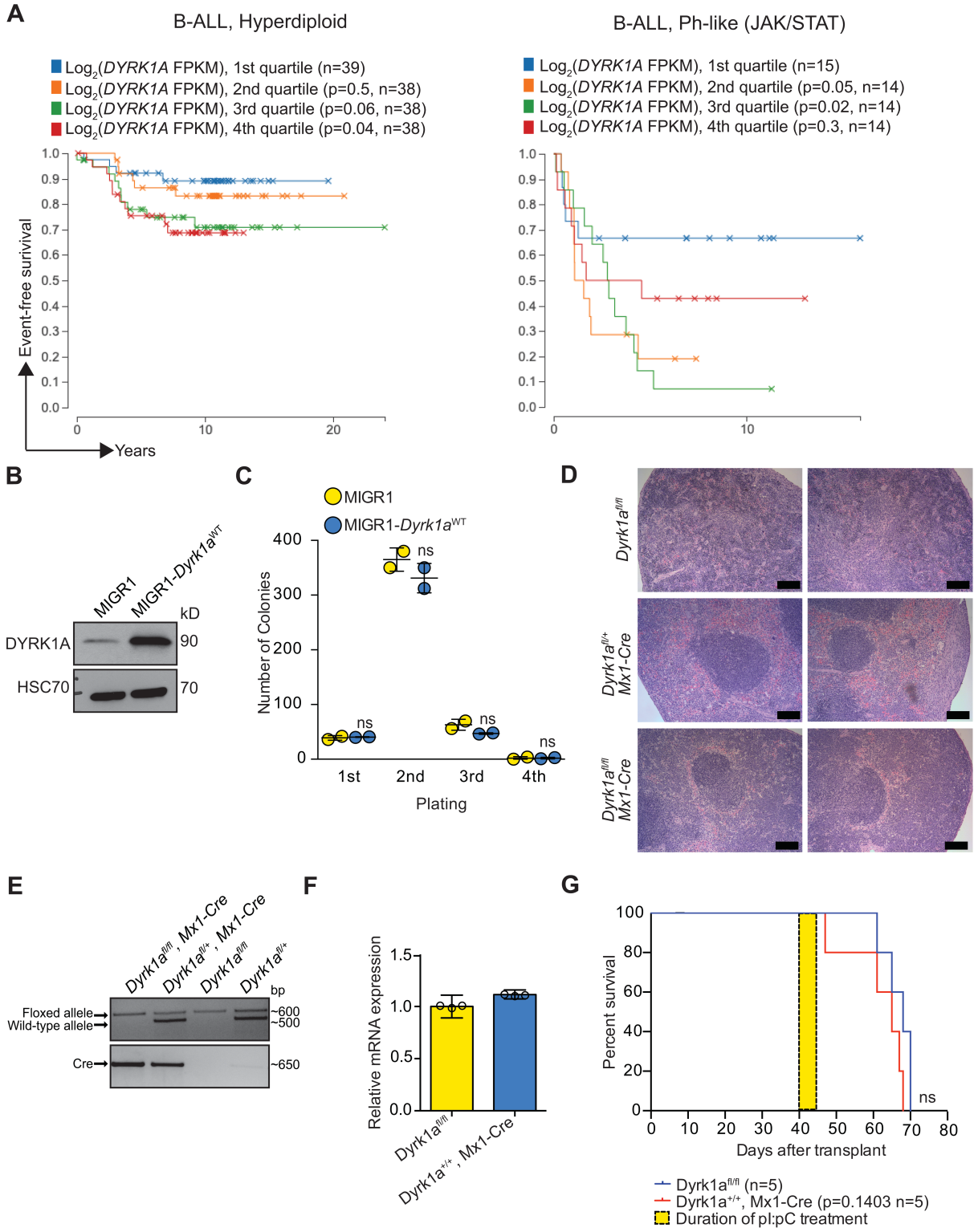

Supplementary Figure S1

Supplementary Figure S1. DYRK1A is required for B-ALL survival in vivo.

(A) Event-free survival analysis from St. Jude GenomePaint Pan-ALL cohort for patients with hyperdiploid (left) or Ph-like (JAK/STAT) (right) B-ALL. Data ordered by quartiles of *DYRK1A* expression. P-values and sample size (n) in panel key.

(B) Western blot showing total DYRK1A protein in Lin^- $B220^+$ cells transduced with MIGR1 or MIGR1-$Dyrk1a^{WT}$. Data representative of 2 biological replicates.

(C) Quantification of colonies during serial replating of cells derived from (B). Mean±SD.

(D) Spleens were harvested from mice described in Figures 1D-F, fixed in formalin, and paraffin-embedded for sectioning and Hematoxylin and Eosin staining. Scale bar: 200µm. Each panel represents a separate mouse per cohort.

(E) BCR-ABL-expressing leukemic cells were isolated from mouse bone marrow once moribund by fluorescence activated cell sorting (FACS) for GFP^+ cells. PCR was performed on genomic DNA from FACS-sorted cells using the primers detailed in Methods section to assess the presence or loss of the targeted allele in $Dyrk1a^{fl/fl}$, $Dyrk1a^{fl/fl}$/*Mx1-Cre* or $Dyrk1a^{fl/+}$, $Dyrk1a^{fl/+}$/*Mx1-Cre* mice.

(F) Mice were transplanted with BCR-ABL (p190) B-ALL cells with $Dyrk1a^{fl/fl}$ or $Dyrk1a^{+/+}$ with *Mx1-Cre* and treated with pI:pC for 2 weeks. Bar chart depicts *Dyrk1a* mRNA expression from qRT-PCR of sorted $CD19^+$ GFP^+ cells from murine bone marrow. CD19 used as a B-cell marker. Mean±SD (from triplicate wells of representative sample).

(G) Kaplan-Meier analysis of mice described in (F). Yellow box represents duration of pI:pC injections (2 weeks). P-values and sample size (n) in panel key.

Significance determined by unpaired *t* test (C) or Log-Rank (Mantel-Cox) test (G). ns, not significant.

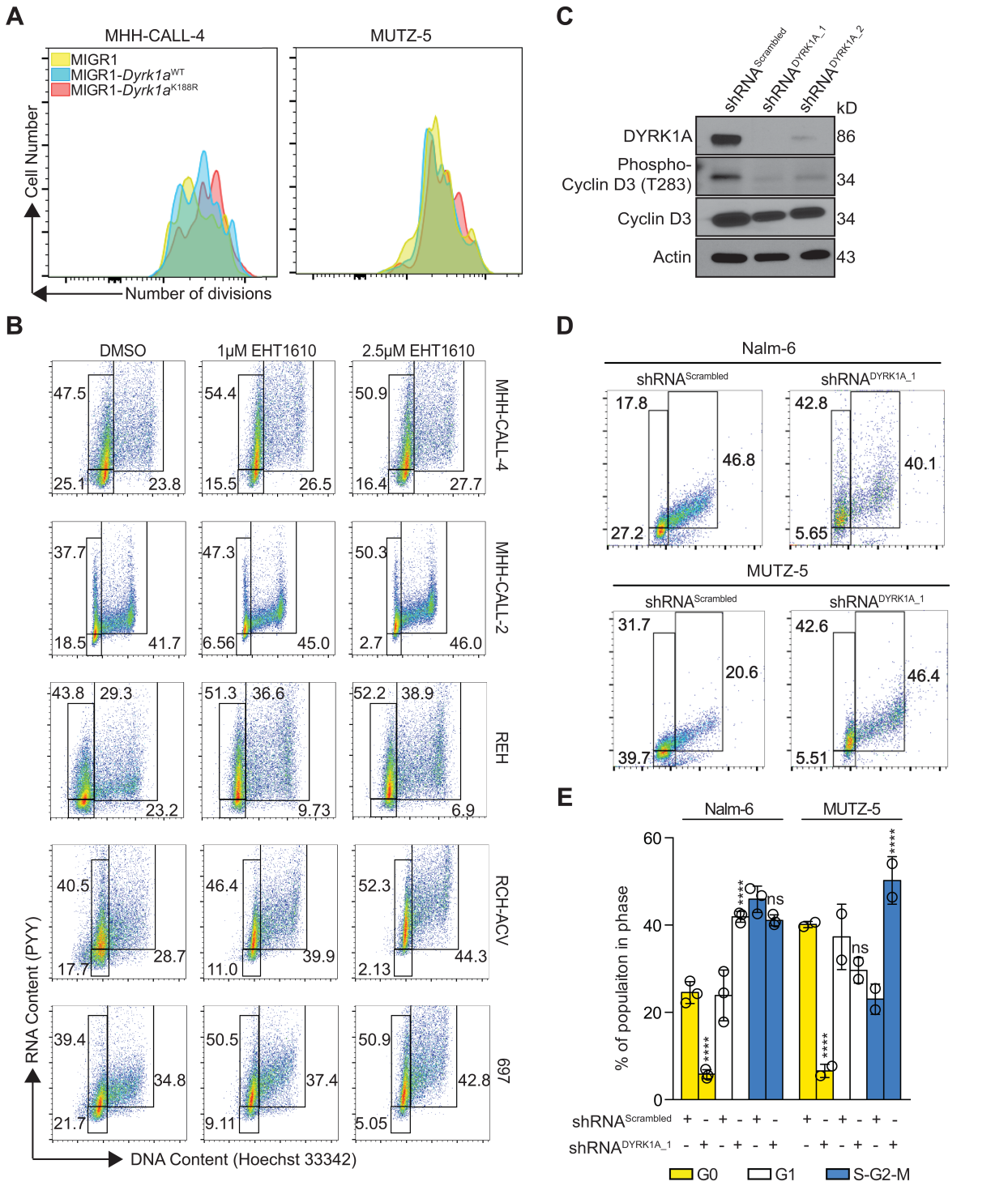

Supplementary Figure S2

Supplementary Figure S2. DYRK1A inhibition impairs B-ALL cell growth.

(A) Representative flow cytometry plot of CellTrace Violet dye dilution assay in GFP^+ cultured B-ALL cell lines transduced with MIGR1, MIGR1-*Dyrk1a*^{WT}, or MIGR1-*Dyrk1a*^{K188R}.

(B) Representative flow cytometry plots of DNA versus RNA content of cell lines after 48-hour treatment with EHT 1610. Numbers indicate percentages in each gate.

(C) Western blot showing DYRK1A, phospho-Cyclin D3 (T283), and total Cyclin D3 protein in MHH-CALL-4 cells transduced with shRNAs (scrambled, DYRK1A_1, DYRK1A_2).

(D) Representative flow cytometry plots of DNA versus RNA content of cell lines after transduction with shRNA^{Scrambled} and shRNA^{DYRK1A_1}. Numbers indicate percentages in each gate.

(E) Cell cycle phase distribution based on gating in (D). Mean±SD. Nalm-6 (n=3 biological replicates), MUTZ-5 (n=2 biological replicates)

(A-C) n=3 biological replicates

Significance determined by ANOVA with post hoc Bonferroni correction (E, compared to scrambled shRNA expression within each cell line). ns, not significant; ****, $p<0.0001$.

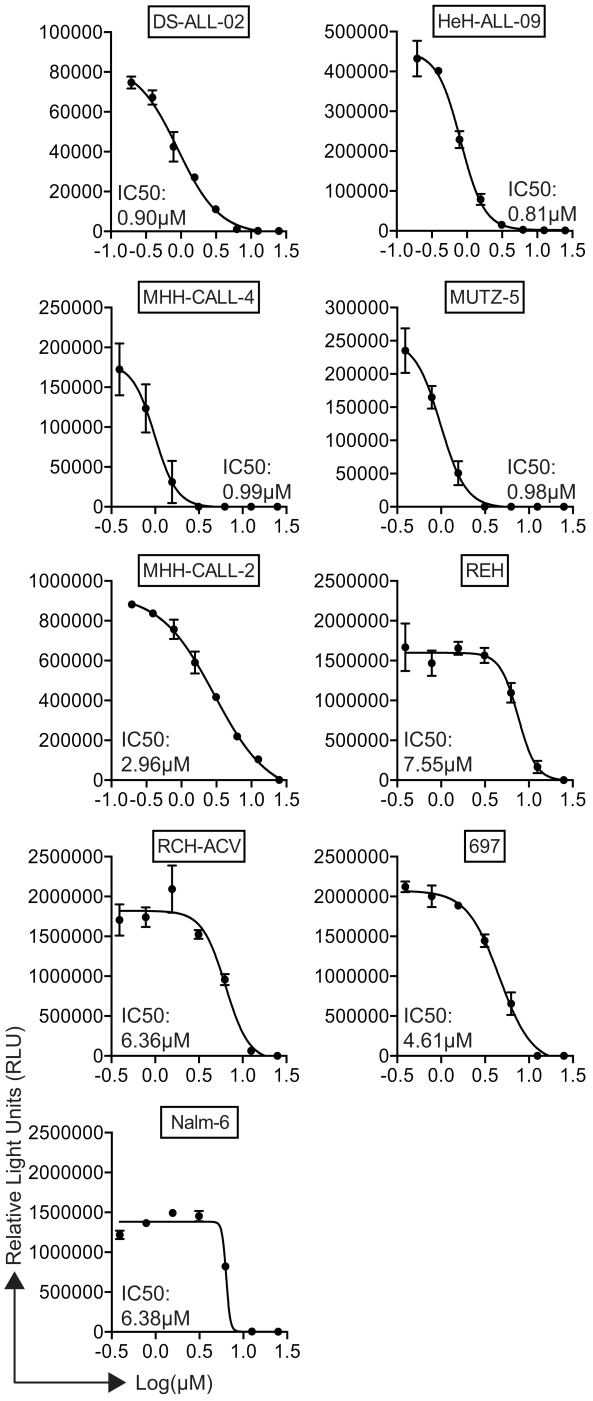

Supplementary Figure S3

Supplementary Figure S3. B-ALL cells are sensitive to EHT 1610 in vitro.

Cell number after treatment with various concentrations of EHT 1610 quantified by luminescence as relative light units (RLUs) from CellTiterGlo 2.0 assays. Curves fitted nonlinearly with variable slope (four parameters). IC50s shown in graph. n=3 biological replicates.

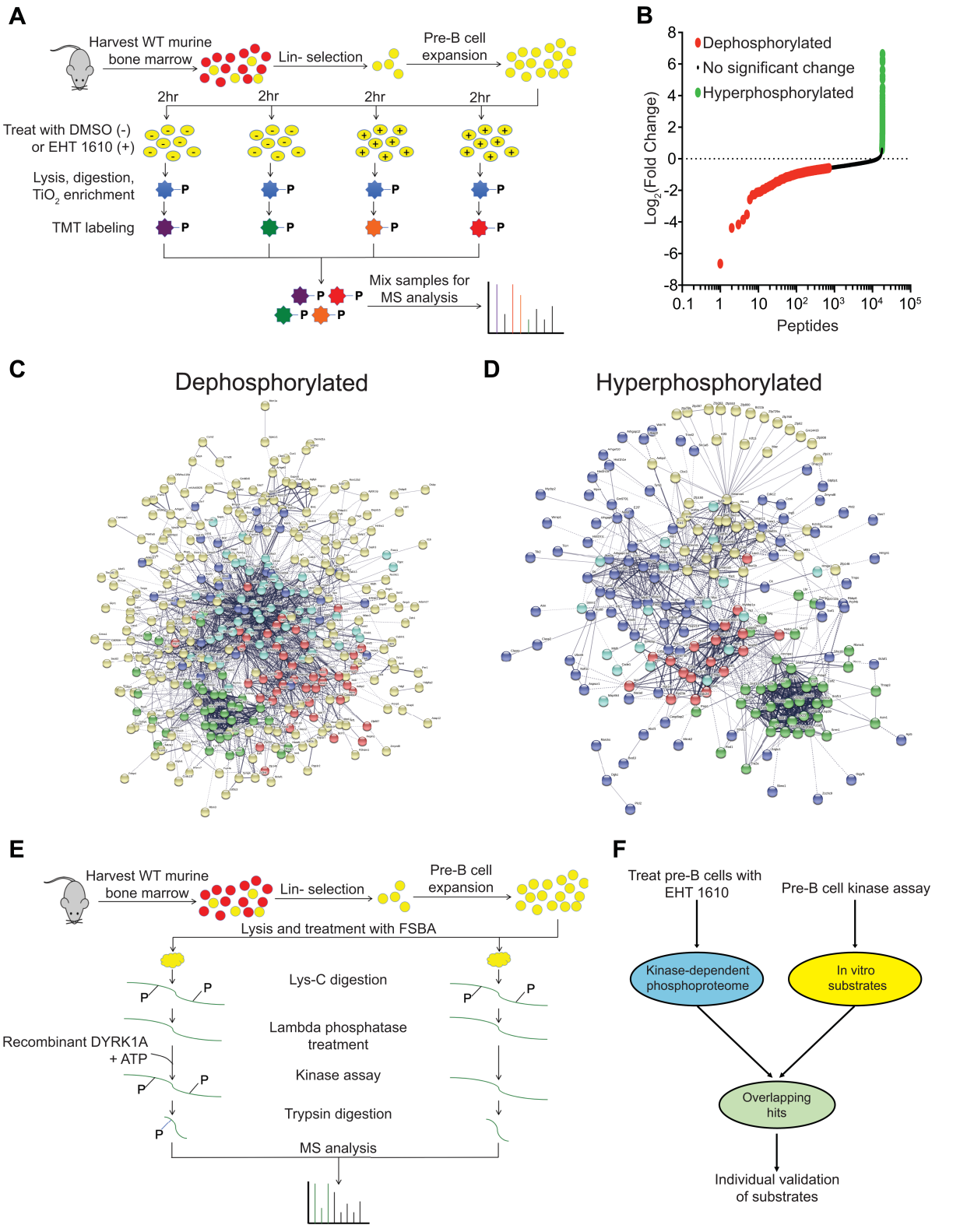

Supplementary Figure S4

Supplementary Figure S4. Kinase assay-linked phosphoproteomics identifies candidate DYRK1A substrates in pre-B cells.

(A) Schematic of global phosphoproteomics assay.

(B) Dot plot of differentially expressed phosphopeptides with hyperphosphorylated (green) and dephosphorylated (red) peptides using a 1.5-fold change cutoff for significance. Peptides were filtered using a false discovery rate (Q) <1% from 2 biological replicates.

(C, D) Redundant phosphopeptides are included in the plot. Interactome analysis was performed using the String database in dephosphorylated (C) and hyperphosphorylated (D) phosphopeptides sets. Disconnected nodes were hidden from the schematic. Colors of nodes represent clustering based on the density of interactions.

(E) Schematic of kinase assay phosphoproteomics. Experiment was performed with 2 biological replicates.

(F) Schematic of strategy used to identify potential DYRK1A substrates from experiments outlined in (A) and (E).

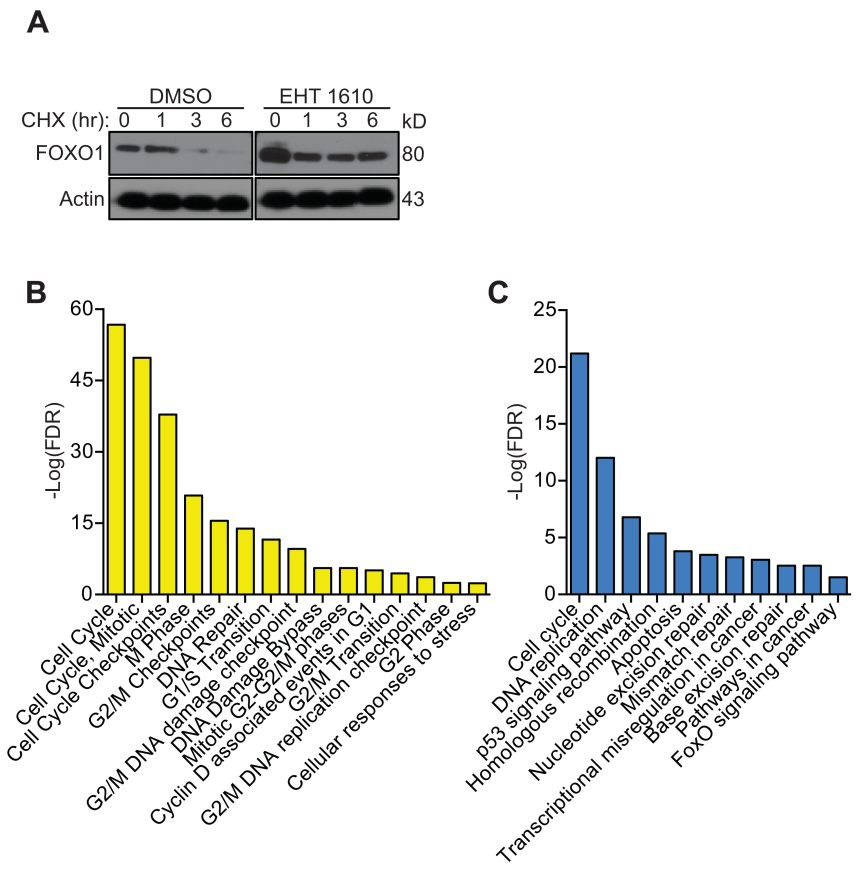

Supplementary Figure S5

Supplementary Figure S5. DYRK1A regulates FOXO1 signaling in late cell cycle and DNA damage response.

(A) Western blot showing total FOXO1 protein in pre-B cells treated with EHT 1610 in the presence of 25µg/mL cycloheximide (CHX). n=3 biological replicates.

(B, C) Upregulated transcripts identified by RNA-sequencing of FACS-sorted small pre-B cells from *Dyrk1a*$^{fl/fl}$ mice with or without *Mx1-Cre(3)* were analyzed in the String Database for Reactome pathway (C) and KEGG pathway (D) enrichment. FDR – False Discovery Rate.

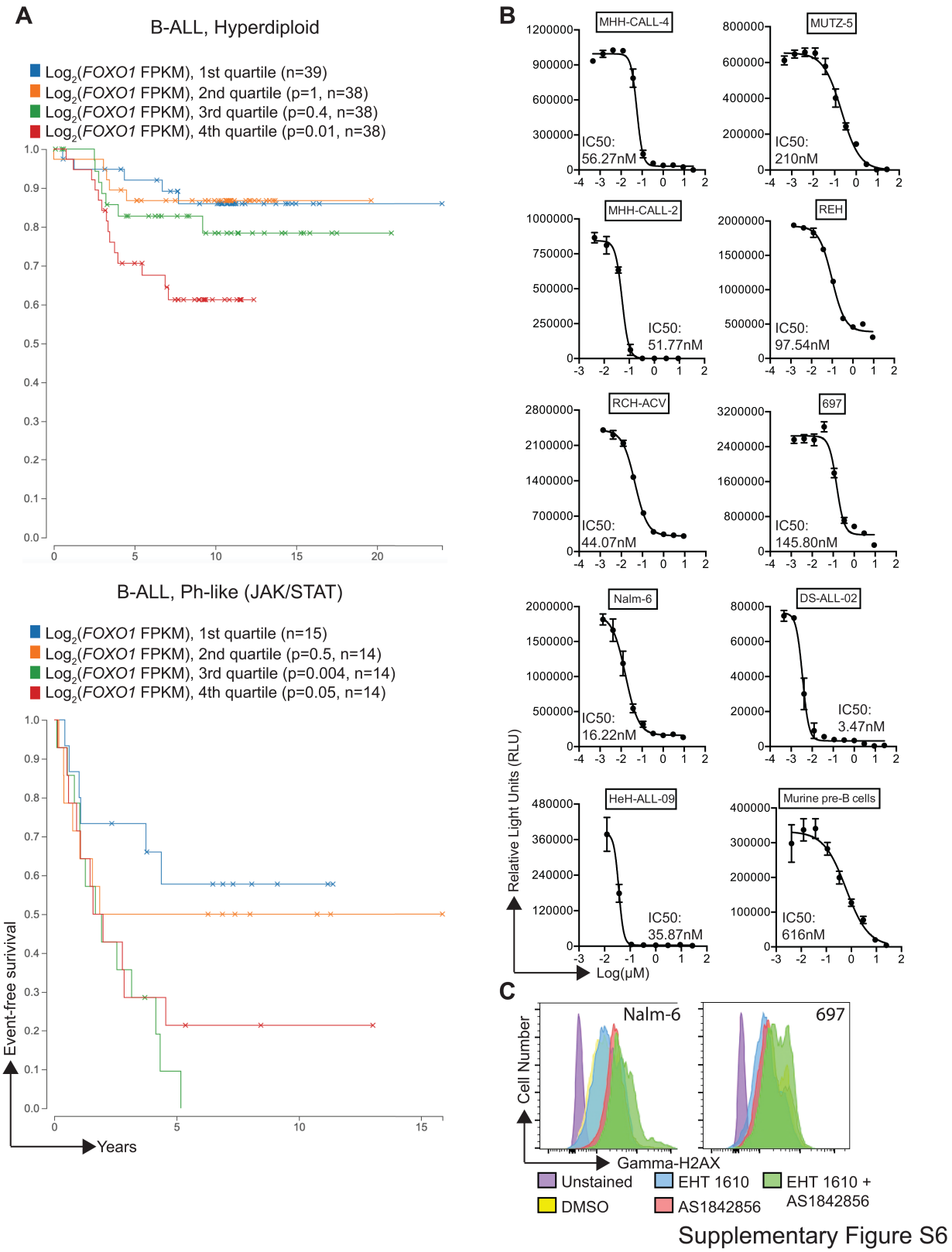

Supplementary Figure S6

Supplementary Figure S6. FOXO1 is required for B-ALL DNA damage response and can be targeted with AS1842856.

(A) Event-free survival analysis from St. Jude GenomePaint Pan-ALL cohort for patients with hyperdiploid (left) or Ph-like (JAK/STAT) (right) B-ALL. Data ordered by quartiles of *FOXO1* expression. P-values and sample size (n) in panel key.

(B) Cell number after treatment with various concentrations of AS1842856 quantified by luminescence as relative light units (RLUs) from CellTiterGlo 2.0 assays. Curves fitted nonlinearly with variable slope (four parameters). IC50s shown in graph.

(C) Representative flow cytometry plots of DNA damage using Gamma-H2AX staining in Nalm-6 and 697 cells treated with EHT 1610, AS1842856 (100nM, 500nM or 1000nM represented by scale bar), or both for 48 hours.

(B, C) n=3 biological replicates.

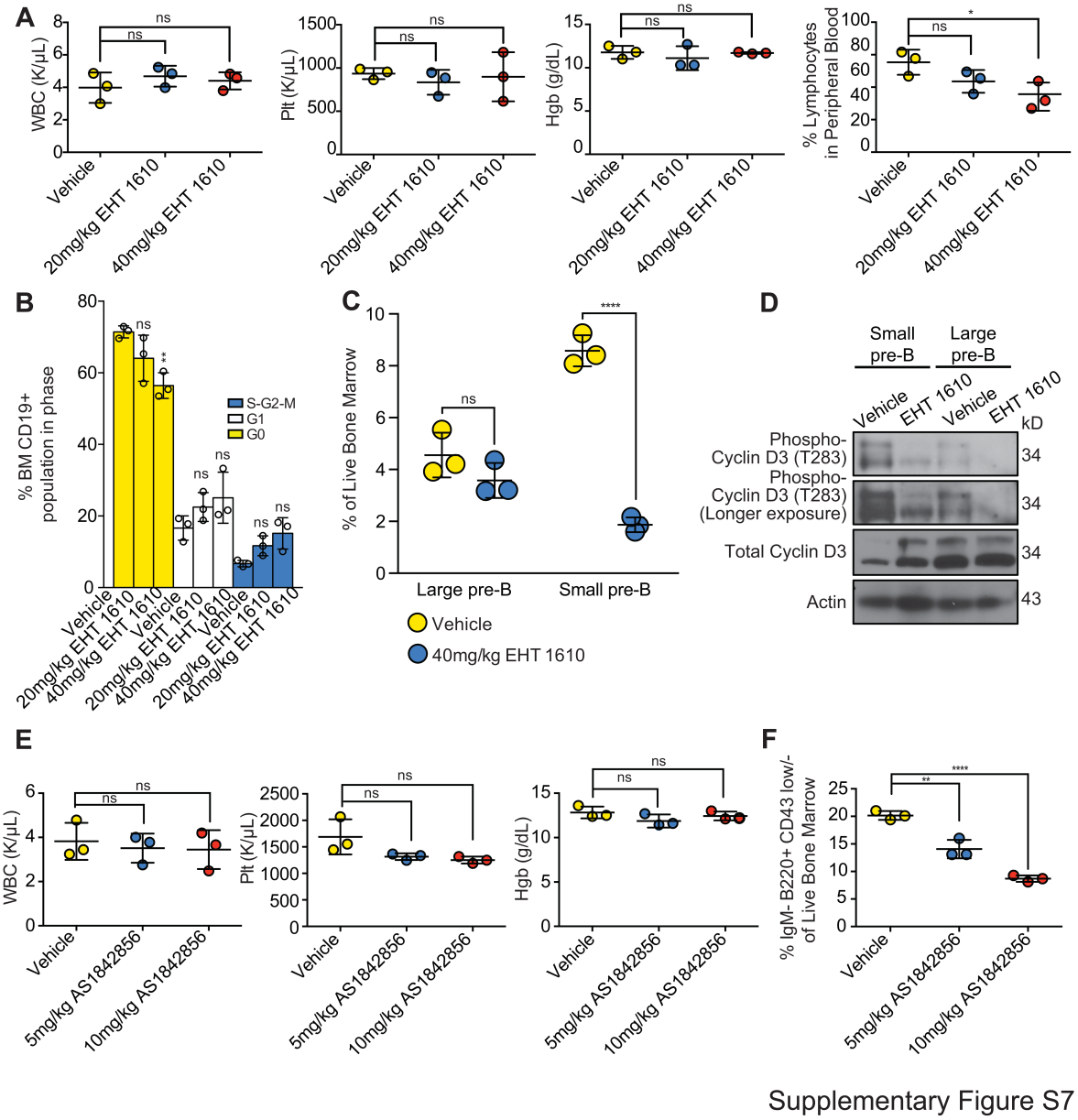

Supplementary Figure S7

Supplementary Figure S7. EHT 1610 and AS1842856 are tolerated in vivo and exhibit on-target effects in C57BL/6 mice.

(A) C57BL/6 mice were injected intraperitoneally with vehicle or EHT 1610 at 20mg/kg/day or 40mg/kg/day for 2 weeks. One day after completing treatment, peripheral blood was collected

for complete blood count (CBC) analysis of white blood cells (WBC), platelets (Plt), hemoglobin (Hgb), and peripheral blood lymphocyte percentage. Mean±SD.

(B) Cell cycle phase distribution of bone marrow $CD19^{+}$ cells from mice described in (A). Mean±SD.

(C-D) C57BL/6 mice were injected intraperitoneally with vehicle or EHT 1610 at 40mg/kg/day for 3 days. Large pre-B (IgM^{-}, $B220^{+}$, $CD43^{low}$, FSC^{high}) and small pre-B (IgM^{-}, $B220^{+}$, $CD43^{-}$, FSC^{low}) cells were isolated using FACS. (C) Comparison of large and small pre-B cell populations between treatment and vehicle groups. Mean±SD. (D) Low-input Western blot for total and phospho-Cyclin D3 (T283) from sorted cells in (C).

(E) C57BL/6 mice were injected intraperitoneally with vehicle or AS1842856 at 5mg/kg/day or 10mg/kg/day for 2 weeks. One day after completing treatment, peripheral blood was collected for CBC analysis of white blood cells (WBC), platelets (Plt), and hemoglobin (Hgb). Mean±SD.

(F) Bone marrow from mice described in (E) was isolated and analyzed for pre-B cells (IgM, $B220^{+}$, $CD43^{low/-}$) by flow cytometry. Mean±SD.

(A-F) n=3 mice per cohort

Significance determined by ANOVA with post hoc Bonferroni correction (A,B,E,F) or unpaired *t* test (C). For B, values compared to vehicle-treated mice within each cohort. ns, not significant; *, $p<0.05$; **, $p<0.01$; ****, $p<0.0001$.

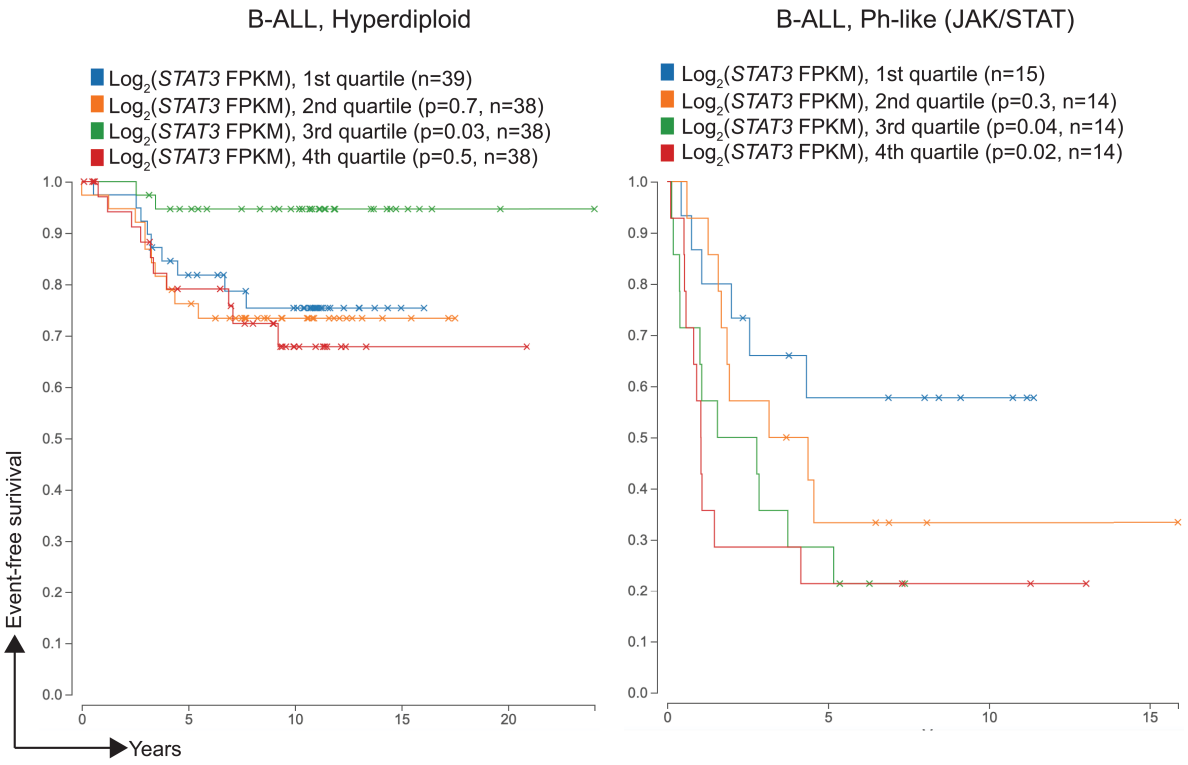

Supplementary Figure S8

Supplementary Figure S8. *STAT3* expression correlates with worse survival outcomes in Ph-like ALL.

(A) Event-free survival analysis from St. Jude GenomePaint Pan-ALL cohort for patients with hyperdiploid (left) or Ph-like (JAK/STAT) (right) B-ALL. Data ordered by quartiles of *STAT3* expression. P-values and sample size (n) in panel key.

Supplementary Tables

Cell Line/PDX Sample	Genetic Background	EHT1610 IC50 (μM)	AS1842856 IC50 (nM)
MHH-CALL-4	Ph-like (*CRLF2, JAK2)*	0.99	56.27
MUTZ-5	Ph-like (*CRLF2, JAK2*)	0.98	210.00
MHH-CALL-2	Hyperdiploid	2.96	51.77
REH	*ETV6-RUNX1*	7.55	97.54
RCH-ACV	*E2A-PBX*	6.36	44.07
Nalm-6	*ETV6-PDGFRB*	6.38	16.22
697	*E2A-PBX*	4.61	145.80
HeH-ALL-09	Hyperdiploid (*KRAS*)	0.81	35.87
DS-ALL-02	Down syndrome-ALL (*CRLF2, JAK2, CDKN2A)*	0.90	3.47
WT Murine Pre-B	C57BL/6J		616.00

Supplementary Table S1. EHT 1610 and AS1842856 IC50 values in B-ALL cell lines and human PDX-passaged B-ALL samples

				EHT1610		Harmine		INDY	
	Patient ID	PDX ID	Risk	IC50 Log[nM]	IC50 µM	IC50 Log[nM]	IC50 µM	IC50 Log[nM]	IC50 µM
B-ALL	ZH61a	m125	VHR	>4.3	>20	>4.3	>20	>4.3	>20
	F18	m1009	VHR	3.397	2.495	3.584	3.837	>4.3	>20
	SN10	m1086	VHR	2.911	0.815	3.631	4.276	4.174	14.928
	L2	m1339	SR	>4.3	>20	4.201	15.885	>4.3	>20
	E55	m1760	SR	>4.3	>20	4.259	18.155	>4.3	>20
T-ALL	N20	m1814	MR	4.2	15.849	>4.3	>20	>4.3	>20
	F110	m2000	HR	>4.3	>20	>4.3	>20	>4.3	>20
	MU46	m3021	MR	>4.3	>20	4.073	11.830	4.228	16.904
	GI33	m1797	MR	>4.3	>20	4.289	19.454	>4.3	>20
	S24	m3013	VHR	2.8	0.631	3.1	1.259	>4.3	>20
DS-ALL	ER43	m1070	VHR	3.846	7.015	3.987	9.705	4.3	20
	M62	m1686	VHR	3.063	1.156	3.754	5.675	3.884	7.656
	DS-FF	m730	MR	3.094	1.242	3.671	4.688	>4.3	>20
	DS-MF	m703	MR	3.877	7.534	4.118	13.122	>4.3	>20
	99-116	m484	MR	3.303	2.009	4.274	18.793	>4.3	>20
	AC23	m39	MR	3.938	8.670	3.862	7.278	>4.3	>20
	DS-GS	m723	MR	>4.3	>20	>4.3	>20	>4.3	>20
	B65	m3285	MR	>4.3	>20	>4.3	>20	4.296	19.770

Supplementary Table S2. EHT 1610, harmine, and INDY IC50 values in ALL patient samples

	Multiples of IC50	EHT1610 (μM)	Cytarabine (μM)	Dexamethasone (μM)	Methotrexate (μM)	AS1842856 (nM)
MHH-CALL-4*	0.25	0.25				14.00
	0.5	0.49				28.00
	1	0.98				56.00
	2	1.96				112.00
	4	3.92				224.00
MUTZ-5*	0.25	0.25				52.50
	0.5	0.49				105.00
	1	0.98				210.00
	2	1.96				420.00
	4	3.92				840.00
MHH-CALL-2*	0.25	0.74				12.94
	0.5	1.48				25.89
	1	2.96				51.77
	2	5.92				103.54
	4	11.84				207.08
REH**	0.25	1.89	0.0071	0.5625		24.38
	0.5	3.77	0.0141	1.1250		48.75
	1	7.55	0.0283	2.2500		97.50
	2	15.10	0.0566	4.5000		195.00
	4	30.20	0.1131	9.0000		390.00
RCH-ACV	0.25	1.59	0.0028	0.0564	0.0030	11.03
	0.5	3.18	0.0056	0.1128	0.0059	22.05
	1	6.36	0.0112	0.2255	0.0118	44.10
	2	12.72	0.0224	0.4510	0.0236	88.20
	4	25.44	0.0448	0.9020	0.0472	176.40
697	0.25	1.15	0.0007	0.0464	0.0028	36.45
	0.5	2.30	0.0014	0.0927	0.0056	72.90
	1	4.61	0.0029	0.1854	0.0112	145.80
	2	9.21	0.0057	0.3708	0.0224	291.60
	4	18.42	0.0115	0.7416	0.0448	583.20
Nalm-6	0.25	1.58	0.0068	0.0592	0.0051	4.05
	0.5	3.17	0.0135	0.1183	0.0103	8.10
	1	6.34	0.0270	0.2366	0.0206	16.20
	2	12.67	0.0540	0.4732	0.0411	32.40
	4	25.35	0.1080	0.9464	0.0823	64.80

*MHH-CALL4, MHH-CALL-2, and MUTZ-5 have sufficient sensitivity towards EHT1610 so cytotoxic chemotherapy synergy assays were not performed with these lines

**REH displayed minimal sensitivity towards Dexamethasone up to 9μM, so multiples up to 9μM were used. REH IC50 to Methotrexate was subnanomolar so this was excluded

Supplementary Table S3. Multiples of IC50 across ALL cell lines for EHT 1610, AS1842856, methotrexate, dexamethasone, and cytarabine

Cell Line:	MHH-CALL-4		MUTZ-5		MHH-CALL-2	
Combination:	EHT+AS		EHT+AS		EHT+AS	
Multiple of IC50	**Fa**	**CI Value**	**Fa**	**CI Value**	**Fa**	**CI Value**
0.25	0.391	0.0842	0.623	0.04838	0.27142	0.30698
0.5	0.422	0.1254	0.71	0.07642	0.594777	0.30482
1	0.523	0.09882	0.834	0.09931	0.782579	0.38568
2	0.819	0.08216	0.883	0.15565	0.938792	0.36833
4	0.93362	0.00188	0.971	0.12759	0.974884	0.45872
Cell Line:	REH					
Combination:	EHT+Dex		EHT+AraC		EHT+AS	
Multiple of IC50	**Fa**	**CI Value**	**Fa**	**CI Value**	**Fa**	**CI Value**
0.25	0.256	0.47982	0.232	0.551	0.31	0.4874
0.5	0.34	0.61691	0.315	0.69824	0.314	0.96232
1	0.437	0.79029	0.386	0.99442	0.675	0.67669
2	0.557	0.93604	0.569	0.888442	0.9	0.49126
4	0.691	1.00172	0.737	0.78482	0.981	0.29382

Cell Line:	RCH-ACV							
Combination:	EHT+Dex		EHT+AraC		EHT+MTX		EHT+AS	
Multiple of IC50	**Fa**	**CI Value**	**Fa**	**CI Value**	**Fa**	**CI Value**	**Fa**	**CI Value**
0.25	0.775	0.32096	0.437	0.50675	0.53095	0.37826	0.3521	0.60819
0.5	0.864	0.53189	0.549	0.88286	0.57396	0.67589	0.42933	0.98548
1	0.981	0.55943	0.73	1.38239	0.71307	0.90939	0.61633	1.20629
2	0.99989	0.22917	0.976	1.20396	0.89618	0.81232	0.88465	0.87718
4	0.99993	0.39901	0.99992	0.4157	0.99886	0.08166	0.99962	0.04011
Cell Line:	Nalm-6							
Combination:	EHT+Dex		EHT+AraC		EHT+MTX		EHT+AS	
Multiple of IC50	**Fa**	**CI Value**	**Fa**	**CI Value**	**Fa**	**CI Value**	**Fa**	**CI Value**
0.25	0.931	0.33054	0.784	0.46473	0.598	0.31439	0.25219	0.74907
0.5	0.992	0.37188	0.981	0.46693	0.688	0.49929	0.41839	0.96146
1	0.99965	0.32974	0.998	0.5186	0.81	0.67872	0.77602	0.76606
2	0.99958	0.69141	0.99979	0.57791	0.982	0.30507	0.99248	0.18188
4	0.99993	0.868889	0.99992	0.89992	0.99914	0.10179	0.99892	0.11635
Cell Line:	697							
Combination:	EHT+Dex		EHT+AraC		EHT+MTX		EHT+AS	
Multiple of IC50	**Fa**	**CI Value**	**Fa**	**CI Value**	**Fa**	**CI Value**	**Fa**	**CI Value**
0.25	0.552	0.47607	0.366	0.61193	0.347	0.40339	0.696	0.14282
0.5	0.673	0.80297	0.561	0.93999	0.402	1.3648	0.752	0.23356
1	0.908	0.95412	0.657	1.64354	0.354	0.78929	0.832	0.32905
2	0.99973	0.2665	0.996	0.65289	0.72	1.0494	0.883	0.48733
4	0.9999	0.38322	0.99994	0.32333	0.977	0.2846	0.914	0.76364

Supplementary Table S4. Combination indices for EHT 1610 combined with cytotoxic chemotherapy or AS1842856

Input	MGI Gene/Marker ID	Symbol	Name
Akap12	MGI:1932576	Akap12	A kinase (PRKA) anchor protein (gravin) 12
Aebp2	MGI:1338038	Aebp2	AE binding protein 2
Mki67	MGI:106035	Mki67	antigen identified by monoclonal antibody Ki 67
Aak1	MGI:1098687	Aak1	AP2 associated kinase 1
Acin1	MGI:1891824	Acin1	apoptotic chromatin condensation inducer 1
Atxn2	MGI:1277223	Atxn2	ataxin 2
Atrx	MGI:103067	Atrx	ATRX, chromatin remodeler
Bin1	MGI:108092	Bin1	bridging integrator 1
C2cd5	MGI:1921991	C2cd5	C2 calcium-dependent domain containing 5
Ccnd3	MGI:88315	Ccnd3	Cyclin D3
Cd44	MGI:88338	Cd44	CD44 antigen
Coro1a	MGI:1345961	Coro1a	coronin, actin binding protein 1A
Cux1	MGI:88568	Cux1	cut-like homeobox 1
Ccnk	MGI:1276106	Ccnk	cyclin K
Dand5	MGI:1344365	Dand5	DAN domain family member 5, BMP antagonist
Dnajc2	MGI:99470	Dnajc2	DnaJ heat shock protein family (Hsp40) member C2
Ezh2	MGI:107940	Ezh2	enhancer of zeste 2 polycomb repressive complex 2 subunit
Eps15	MGI:104583	Eps15	epidermal growth factor receptor pathway substrate 15
Etv6	MGI:109336	Etv6	ets variant 6
Eif4g1	MGI:2384784	Eif4g1	eukaryotic translation initiation factor 4, gamma 1
Eif4b	MGI:95304	Eif4b	eukaryotic translation initiation factor 4B
Eif4ebp1	MGI:103267	Eif4ebp1	eukaryotic translation initiation factor 4E binding protein 1
Foxk1	MGI:1347488	Foxk1	forkhead box K1
Foxo1	MGI:1890077	Foxo1	forkhead box O1
Gpkow	MGI:1859610	Gpkow	G patch domain and KOW motifs
Gatad2a	MGI:2384585	Gatad2a	GATA zinc finger domain containing 2A
Gtf2f1	MGI:1923848	Gtf2f1	general transcription factor IIF, polypeptide 1
Git1	MGI:1927140	Git1	GIT ArfGAP 1
Glcci1	MGI:2179717	Glcci1	glucocorticoid induced transcript 1
Hsp90ab1	MGI:96247	Hsp90ab1	heat shock protein 90 alpha (cytosolic), class B member 1
Huwe1	MGI:1926884	Huwe1	HECT, UBA and WWE domain containing 1
Hnrnpk	MGI:99894	Hnrnpk	heterogeneous nuclear ribonucleoprotein K
Htatsf1	MGI:1919709	Htatsf1	HIV TAT specific factor 1
Hcfc1	MGI:105942	Hcfc1	host cell factor C1
Ibtk	MGI:1918677	Ibtk	inhibitor of Bruton agammaglobulinemia tyrosine kinase
Ifngr1	MGI:107655	Ifngr1	interferon gamma receptor 1

Iws1	MGI:1920723	Iws1	IWS1, SUPT6 interacting protein
jmjd1c	MGI:1918614	Jmjd1c	jumonji domain containing 1C
Kansl1	MGI:1923969	Kansl1	KAT8 regulatory NSL complex subunit 1
Larp1	MGI:1890165	Larp1	La ribonucleoprotein domain family, member 1
Larp4	MGI:2443114	Larp4	La ribonucleoprotein domain family, member 4
Leo1	MGI:2685031	Leo1	Leo1, Paf1/RNA polymerase II complex component
Lrrfip1	MGI:1342770	Lrrfip1	leucine rich repeat (in FLII) interacting protein 1
Lsp1	MGI:96832	Lsp1	lymphocyte specific 1
Kdm6a	MGI:1095419	Kdm6a	lysine (K)-specific demethylase 6A
Med15	MGI:2137379	Med15	mediator complex subunit 15
Mettl3	MGI:1927165	Mettl3	methyltransferase like 3
Mef2d	MGI:99533	Mef2d	myocyte enhancer factor 2D
Myo9b	MGI:106624	Myo9b	myosin IXb
Nedd4l	MGI:1933754	Nedd4l	neural precursor cell expressed, developmentally down-regulated gene 4-like
Nipbl	MGI:1913976	Nipbl	NIPBL cohesin loading factor
Nfrkb	MGI:2442410	Nfrkb	nuclear factor related to kappa B binding protein
Numa1	MGI:2443665	Numa1	nuclear mitotic apparatus protein 1
Ncor1	MGI:1349717	Ncor1	nuclear receptor co-repressor 1
Ncor2	MGI:1337080	Ncor2	nuclear receptor co-repressor 2
Npm1	MGI:106184	Npm1	nucleophosmin 1
Pds5a	MGI:1918771	Pds5a	PDS5 cohesin associated factor A
Pnn	MGI:1100514	Pnn	pinin
Pkp4	MGI:109281	Pkp4	plakophilin 4
Pnisr	MGI:1913875	Pnisr	PNN interacting serine/arginine-rich
Ptbp3	MGI:1923334	Ptbp3	polypyrimidine tract binding protein 3
Prrc2c	MGI:1913754	Prrc2c	proline-rich coiled-coil 2C
Prkd3	MGI:1922542	Prkd3	protein kinase D3
Pkn1	MGI:108022	Pkn1	protein kinase N1
Ppp1r7	MGI:1913635	Ppp1r7	protein phosphatase 1, regulatory subunit 7
Ppp1r9b	MGI:2387581	Ppp1r9b	protein phosphatase 1, regulatory subunit 9B
Ptprc	MGI:97810	Ptprc	protein tyrosine phosphatase, receptor type, C
Pum1	MGI:1931749	Pum1	pumilio RNA-binding family member 1
Reps1	MGI:1196373	Reps1	RalBP1 associated Eps domain containing protein
Ranbp3	MGI:1919060	Ranbp3	RAN binding protein 3
Rasgrp2	MGI:1333849	Rasgrp2	RAS, guanyl releasing protein 2
Rcsd1	MGI:2676394	Rcsd1	RCSD domain containing 1
Rgcc	MGI:1913464	Rgcc	regulator of cell cycle
Rsf1	MGI:2682305	Rsf1	remodeling and spacing factor 1
Rfc1	MGI:97891	Rfc1	replication factor C (activator 1) 1
Arhgef7	MGI:1860493	Arhgef7	Rho guanine nucleotide exchange factor (GEF7)
Arhgef2	MGI:103264	Arhgef2	rho/rac guanine nucleotide exchange factor (GEF) 2

Rrm2	MGI:98181	Rrm2	ribonucleotide reductase M2
Rpl6	MGI:108057	Rpl6	ribosomal protein L6
Ric8a	MGI:2141866	Ric8a	RIC8 guanine nucleotide exchange factor A
Rnf213	MGI:1289196	Rnf213	ring finger protein 213
Rbm14	MGI:1929092	Rbm14	RNA binding motif protein 14
Rbm27	MGI:2147194	Rbm27	RNA binding motif protein 27
Rbm5	MGI:1933204	Rbm5	RNA binding motif protein 5
Sltm	MGI:1913910	Sltm	SAFB-like, transcription modulator
Samsn1	MGI:1914992	Samsn1	SAM domain, SH3 domain and nuclear localization signals, 1
Srrm1	MGI:1858303	Srrm1	serine/arginine repetitive matrix 1
Srrm2	MGI:1923206	Srrm2	serine/arginine repetitive matrix 2
Srsf1	MGI:98283	Srsf1	serine/arginine-rich splicing factor 1
Srsf2	MGI:98284	Srsf2	serine/arginine-rich splicing factor 2
Set	MGI:1860267	Set	SET nuclear oncogene
Stat3	MGI:103038	Stat3	signal transducer and activator of transcription 3
Slc19a1	MGI:103182	Slc19a1	solute carrier family 19 (folate transporter), member 1
Slc25a1	MGI:1345283	Slc25a1	solute carrier family 25 (mitochondrial carrier, citrate transporter), member 1
Sf3b1	MGI:1932339	Sf3b1	splicing factor 3b, subunit 1
Sf3b2	MGI:2441856	Sf3b2	splicing factor 3b, subunit 2
Sympk	MGI:1915438	Sympk	symplekin
Synrg	MGI:1354742	Synrg	synergin, gamma
Taf3	MGI:2388097	Taf3	TATA-box binding protein associated factor 3
Tmpo	MGI:106920	Tmpo	thymopoietin
Thrap3	MGI:2442637	Thrap3	thyroid hormone receptor associated protein 3
Top2a	MGI:98790	Top2a	topoisomerase (DNA) II alpha
Top2b	MGI:98791	Top2b	topoisomerase (DNA) II beta
Tfeb	MGI:103270	Tfeb	transcription factor EB
Tcof1	MGI:892003	Tcof1	treacle ribosome biogenesis factor 1
U2surp	MGI:1915208	U2surp	U2 snRNP-associated SURP domain containing
Uhrf1	MGI:1338889	Uhrf1	ubiquitin-like, containing PHD and RING finger domains, 1
Ybx1	MGI:99146	Ybx1	Y box protein 1
Yeats2	MGI:2447762	Yeats2	YEATS domain containing 2

Supplementary Table S5. 109 overlapping phosphopeptides from global and kinase assay phosphoproteomics

GO Biological Process	False Discovery Rate (FDR)
gene expression	1.41E-12
nucleic acid metabolic process	1.70E-12
macromolecule biosynthetic process	4.11E-12
regulation of nitrogen compound metabolic process	4.11E-12
regulation of gene expression	1.19E-11
cellular macromolecule biosynthetic process	1.19E-11
RNA metabolic process	1.66E-11
cellular nitrogen compound metabolic process	1.88E-11
cellular nitrogen compound biosynthetic process	5.14E-11
regulation of RNA metabolic process	9.13E-11
regulation of cellular biosynthetic process	1.10E-10
nucleobase-containing compound metabolic process	1.37E-10
cellular macromolecule metabolic process	1.37E-10
regulation of nucleobase-containing compound metabolic process	2.40E-10
regulation of macromolecule biosynthetic process	2.70E-10
transcription, DNA-templated	3.35E-10
regulation of cellular macromolecule biosynthetic process	3.65E-10
macromolecule metabolic process	9.57E-10
nucleobase-containing compound biosynthetic process	1.37E-09
regulation of metabolic process	1.46E-09
regulation of macromolecule metabolic process	1.83E-09
regulation of primary metabolic process	1.87E-09
regulation of cellular metabolic process	2.11E-08
regulation of transcription from RNA polymerase II promoter	7.71E-08
negative regulation of nitrogen compound metabolic process	0.000000188
chromosome organization	0.00000113
negative regulation of nucleobase-containing compound metabolic process	0.00000122
regulation of cellular process	0.00000217
cellular process	0.00000249
negative regulation of cellular process	0.00000249
negative regulation of macromolecule metabolic process	0.00000249

primary metabolic process	0.00000249
negative regulation of cellular metabolic process	0.0000025
cellular metabolic process	0.0000025
negative regulation of cellular macromolecule biosynthetic process	0.00000269
regulation of mRNA processing	0.00000304
negative regulation of gene expression	0.00000419
negative regulation of RNA metabolic process	0.00000562
organic substance metabolic process	0.00000668
organelle organization	0.00000892
mRNA processing	0.0000129
chromatin organization	0.0000144
positive regulation of cellular process	0.0000165
positive regulation of metabolic process	0.000022
positive regulation of biological process	0.0000282
regulation of biological process	0.000037
cellular component organization	0.0000521
regulation of mRNA splicing, via spliceosome	0.0000619
biological regulation	0.0000722
RNA splicing	0.0000941
positive regulation of macromolecule metabolic process	0.0000969
positive regulation of cellular metabolic process	0.000101
metabolic process	0.00011
RNA processing	0.000127
negative regulation of transcription from RNA polymerase II promoter	0.000134
chromatin modification	0.000162
negative regulation of transcription, DNA-templated	0.000162
cell cycle process	0.000283
positive regulation of transcription from RNA polymerase II promoter	0.000297
positive regulation of transcription, DNA-templated	0.000348
regulation of cell cycle	0.000417
positive regulation of cellular biosynthetic process	0.000425
cell cycle	0.000435

positive regulation of nitrogen compound metabolic process	0.000462
negative regulation of mRNA splicing, via spliceosome	0.00055
positive regulation of gene expression	0.000969
single-organism organelle organization	0.00104
transcription from RNA polymerase II promoter	0.00134
positive regulation of macromolecule biosynthetic process	0.00155
negative regulation of cell cycle	0.00177
single-organism developmental process	0.00201
hematopoietic or lymphoid organ development	0.00201
regulation of cellular component organization	0.00228
positive regulation of nucleobase-containing compound metabolic process	0.00241
anatomical structure development	0.00264
immune system development	0.00289
biological_process	0.00313
erythrocyte differentiation	0.00338
histone modification	0.00446
TOR signaling	0.00519
homeostasis of number of cells	0.00535
immune system process	0.00535
DNA metabolic process	0.0062
positive regulation of protein deacetylation	0.00884
positive regulation of protein metabolic process	0.00975
DNA replication	0.0101
mitotic cell cycle process	0.0108
DNA conformation change	0.0114
cell differentiation	0.013
cellular developmental process	0.0136
positive regulation of cellular protein metabolic process	0.0136
regulation of lipid transport by regulation of transcription from RNA polymerase II promoter	0.0137
mitotic cell cycle	0.014
nuclear division	0.014
regulation of cell cycle process	0.014

response to osmotic stress	0.0144
regulation of organelle organization	0.015
positive regulation of protein modification process	0.0153
translational initiation	0.0161
single-multicellular organism process	0.0173
hemopoiesis	0.0173
multicellular organismal development	0.0189
system development	0.0191
DNA packaging	0.0198
apoptotic chromosome condensation	0.0204
cellular response to stimulus	0.0204
regulation of transcription elongation from RNA polymerase II promoter	0.0204
lung development	0.0264
positive regulation of DNA metabolic process	0.0281
respiratory tube development	0.0283
chromosome segregation	0.0289
tube development	0.0436
in utero embryonic development	0.0468
histone ubiquitination	0.048
single-organism cellular process	0.0495

Supplementary Table S6. Enriched GO Biological Processes in 109 overlapping phosphopeptides

			AS1842856		Idarubicin	
	Patient ID	**PDX ID**	**IC50 Log[nM]**	**IC50(nm)**	**IC50 Log[nM]**	**IC50(nM)**
DS-ALL	DS-2818	124	2.18	151.36	0.56	3.63
	DS-ALL01	365	1.96	91.11	2.03	106.39
	DS-16013	408	2.28	191.57	1.98	95.17
	DS-4366	1450	2.23	171.45	0.90	7.88
HeH-ALL	DOS	148	1.69	48.76	0.51	3.23
	HD-21093	859	2.78	607.88	1.81	63.91
	HD-14207	881	1.86	72.70	1.89	77.35
	HD-12206	907	2.58	378.74	1.75	56.64
	HD-18082	909	2.26	180.13	1.39	24.62
B-ALL (Other)	F18	m1009	2.27	188.14	0.72	5.24
	SN10	m1086	1.83	67.48	0.57	3.71
	ZH61a	m1225	2.06	115.46	0.69	4.95
	L2	m1339	2.80	627.42	0.71	5.19
	E55	m1759	2.22	167.40	0.72	5.21

Supplementary Table S7. AS1842856 and Idarubicin IC50 values in ALL patient cells

PDX Sample ID	Alias	Tumor Type	Tumor Subtype	Patient Age	Driving Lesion	Other Gene Alterations
SJBALL021964_D1	TB-10-1926	B-ALL	Ph-like	6	P2RY8-CRLF2	EBF1, IKZF1, RAG1/2, BTG1
SJBALL265_D1	PANNGL	B-ALL	Ph-like	12	PAX5-JAK2	IKZF1, SETD2

Supplementary Table S8. Background information of human PDX-passaged Ph-like ALL samples

Antigen	Source	Clone	Catalog number
Antibodies used for flow cytometry			
B220	BD	RA3-6B2	553087
CD43	BD	S7	562866
IgM	eBioscience	II/41	48-5790-82
CD19	eBioscience	eBio1D3	17-0193-82
Annexin V	BD	DX2	556421
CD19 (human)	eBioscience	HIB19	25-0199-42
CD45 (human)	eBioscience	2D1	17-9459-42
Gamma-H2AX	BD	N1-431	560447
Phospho-CDK1 (phospho-cdc2) Y15	Cell Signaling Technology	10A11	4539S
Rabbit IgG	Abcam	Polyclonal	Ab175470
Antibodies used for Western blotting			
DYRK1A	Abnova	7D10	H00001859-M01
Cyclin D3	Santa Cruz Biotechnology	C-16	sc-182-G
Phospho-Cyclin D3 T283	Abcam	Polyclonal	ab55322
Phospho-Cyclin D3 T283	Cell Signaling Technology	E1V6W	53966S
FOXO1	Cell Signaling Technology	C29H4	2880, 76764
Phospho-FOXO1 S329	Aviva Systems Biology	Polyclonal	OAAF07382-Biotin
TBP	Cell Signaling Technology	D5C9H	44059
STAT3	Cell Signaling Technology	124H6	9139S
Phospho-STAT3 Y705	Cell Signaling Technology	D3A7	9145, 4093
Phospho-STAT3 S727	Cell Signaling Technology	D8C2Z	49081S
HSC70	Santa Cruz Biotechnology	B-6	sc-7298
Beta-Actin	Santa Cruz Biotechnology	C4	sc-47778
Rabbit IgG (HRP-conjugated)	GE Healthcare	Polyclonal	NA934
Mouse IgG (HRP-conjugated)	GE Healthcare	Polyclonal	NA931
Biotin (HRP-conjugated)	ThermoFisher Scientific	N/A	SA10001
Biotin (IRDye 680RD Streptavidin)	LI-COR	N/A	68079
Biotin (IRDye 800CW Streptavidin)	LI-COR	N/A	32230
Rabbit IgG (IRDye 680RD)	LI-COR	Polyclonal	68071
Mouse IgG (IRDye 800CW)	LI-COR	Polyclonal	32213
Anti-thiophosphate ester	Abcam	51-8	ab92570
Anti-mouse lineage panel			
CD3	BioLegend	145-2C11	133307
Ly-6G/Ly-6C		RB6-8C5	
CD11b		M1/70	
CD45R		RA3-6B2	
TER-119		Ter-119	

Supplementary Table S9. Antibody information